Vibrationally resolved spectra of C2–C11 by anion photoelectron spectroscopy

D. W. Arnold, S. E. Bradforth, T. N. Kitsopoulos, and D. M. Neumark

Citation: The Journal of Chemical Physics **95**, 8753 (1991); doi: 10.1063/1.461211
View online: http://dx.doi.org/10.1063/1.461211
View Table of Contents: http://scitation.aip.org/content/aip/journal/jcp/95/12?ver=pdfcov
Published by the AIP Publishing

Vibrationally resolved spectra of C_2–C_{11} by anion photoelectron spectroscopy

D. W. Arnold,[a] S. E. Bradforth, T. N. Kitsopoulos, and D. M. Neumark[b]
Department of Chemistry, University of California, Berkeley, California 94720

(Received 9 July 1991; accepted 3 September 1991)

Anion photoelectron spectroscopy has been employed to obtain vibrationally resolved spectra of the carbon molecules C_2–C_{11}. The spectra of C_2^-–C_9^- are dominated by linear anion to linear neutral photodetachment transitions. Linear to linear transitions contribute to the C_{11}^- spectrum, as well. From these spectra, vibrational frequencies and electron affinities are determined for the linear isomers of C_2–C_9 and C_{11}. The term value is also obtained for the first excited electronic state of linear C_4. The spectra of C_{10}^- and C_{11}^- show evidence for transitions involving cyclic anions and/or neutrals. Similar types of transitions are identified in the spectra of other smaller molecules, specifically C_6^-, C_8^-, and to a lesser extent C_5^-.

I. INTRODUCTION

For several decades researchers have studied pure carbon molecules, attempting to elucidate their physical properties and the processes governing their formation. Carbon molecules have been identified as intermediates in soot formation,[1] they exist in the vapor above heated graphite,[2] and they have been detected in interstellar space,[3] being produced in giant carbon stars. Recently, the verification of the icosahedral structure of the C_{60} molecule[4,5] has launched a new investigation of the formation processes of such novel cage structures. An excellent review of the vast amount of research performed on carbonaceous species through April 1989 has been given by Weltner and van Zee.[6] Given the abundance of research on these molecules, surprisingly little is definitely known about the physical properties of pure carbon molecules containing more than three atoms. Before a model for the formation of the large complexes such as the fullerenes and soot can be fully developed, fundamental information about the building block carbon molecules must be compiled. Determination of the molecular properties of the smaller carbon molecules and how these properties change with molecular size should provide a more complete understanding of these processes.

One of the more controversial issues encountered in carbon molecule research is the determination of the lowest energy molecular geometries. Until recently, this question was addressed mainly by *ab initio* calculations. Early molecular orbital (MO) calculations by Pitzer and Clementi[7] and Hoffman[8] predicted that the carbon molecules would have cumulenic linear structures until reaching the size of C_{10}, at which time the energy stabilization gained by the formation of an additional bond would be larger than the destabilization created by ring strain and it would form a monocyclic ring. Recent experiments by Saykally, Bernath, Amano, and co-workers[3,9,10,11] as well as calculations at higher levels of theory[12,13] have confirmed this hypothesis for the *odd*-numbered carbon molecules (up to C_9), finding linear $D_{\infty h}$ geometries for the $^1\Sigma_g^+$ ground state of each of these species.[13,14] However, calculations predict that planar monocyclic ^1A_g isomers exist for even-numbered carbon molecules as small as C_4, with energies near those of the linear $^3\Sigma_g^-$ species. The relative energies of the two forms vary depending upon the level of the calculation, and the energy separations are often less than the error limits of the calculations. Even very high levels of *ab initio* theory predict that the cyclic forms of these molecules may be energetically more stable than their linear counterparts.[15] However, calculations considering entropic effects have shown that the high temperatures of natural formation conditions thermodynamically favor linear carbon molecules over their nonlinear counterparts.[16]

Most quantitative experimental information about carbon molecules containing more than three atoms has been obtained during the last five years. Researchers have employed electron-spin resonance (ESR) techniques to detect the linear forms of several even-numbered species in low-temperature matrices.[17] Yang *et al.*[18,19] used anion photoelectron spectroscopy to obtain electron affinities and electronic structure for carbon molecules with up to 84 carbon atoms. They deduced that they were observing the linear forms of C_n ($n = 2$–9) and monocyclic ring forms of C_n ($n = 10$–29). Absorption experiments have been performed, both in matrices and in the gas phase. However, conclusive assignment of spectral peaks is often difficult due to the presence of multiple species with varying numbers of carbon atoms. As a result, several bands originally assigned in matrix isolation spectroscopy[20] have necessarily been reassigned by techniques which are more molecule-specific. Isotope studies in matrices have clearly assigned vibrational frequencies for the linear forms of C_4,[21] C_5,[22] and C_6.[23] High resolution gas-phase spectra have been obtained for linear forms of C_4,[24] C_5,[10] C_7,[11] and C_9,[14] yielding rotational constants and at least one vibrational frequency for each.[25] While most experimentalists studying carbon molecules with less than ten atoms have detected only the linear forms of the molecules, evidence for nonlinear isomers has been obtained by researchers using the Coulomb explosion imaging (CEI) technique, who reported the photodetachment of cyclic forms of C_4^-, C_5^-, and C_6^-.[26]

Using an anion photoelectron spectroscopy technique

[a] National Science Foundation Predoctoral Fellow.
[b] National Science Foundational Presidential Young Investigator and Alfred P. Sloan Fellow.

similar to that of Yang *et al.*,[18] but at considerably higher resolution, we have obtained vibrationally resolved photoelectron spectra of the anions C_2^-–C_{11}^-. The use of an anion precursor allows study of the single mass-selected neutral molecule of interest, circumventing chromophore uncertainties encountered in absorption experiments. The photoelectron experiment also complements infrared absorption experiments by providing vibrational frequencies which are infrared inactive. In addition, since anion photodetachment is a vertical process, the length of the observed vibrational progression provides information about the difference in geometry between the anion and the neutral. The spectra presented here, with the exception of C_{10}^-, show evidence for transitions between linear carbon anions and linear carbon neutrals. Electron affinities (EAs) are measured for all the linear carbon molecules. Vibrational frequencies are determined for many of the linear neutral carbon species and an excited electronic state is assigned for C_4. In addition, the photoelectron spectra of C_{10}^- and C_{11}^-, and to a lesser extent those of C_5^-, C_6^-, and C_8^-, show contributions from what are believed to be nonlinear isomers of the carbon anions. The structures of the nonlinear anions cannot be determined from these spectra, but it is apparent that photodetachment of these anions results in a significant geometrical reorganization of the neutral.

II. EXPERIMENTAL

The apparatus used in these experiments is a modified version of our previously described anion time-of-flight photoelectron spectrometer.[27] Carbon anions are generated in a Smalley-type laser vaporization/pulsed molecular beam source.[28] A XeCl excimer laser is focused onto a rotating and translating graphite rod (0.25 in. diam). The resulting plasma is swept through a 1 cm long, 0.25 cm diam channel by helium carrier gas pulsed from a molecular beam valve (General Valve Series 9), operated at a backing pressure of ~5 atm. The gas mixture expands, allowing relaxation of molecular vibrations and rotations by collisions with the carrier gas atoms. The anions generated in the plasma are injected into a Wiley–McLaren-type time-of-flight mass spectrometer[29] with a pulsed electric field. After acceleration to an energy of 1 keV, the ions separate out by mass and are detected by a microchannel plate detector. The mass resolution of the instrument, $M/\Delta M$, is ~150. The ion of interest is selectively detached by a properly timed pulse of light from a pulsed Nd:YAG photodetachment laser. After photodetachment, a dual microchannel plate detector at the end of a 1 m field-free flight tube detects a small fraction (≈0.01%) of the detached electrons. Time-of-flight analysis yields electron kinetic energies (eKE); the instrumental resolution is 8 meV at 0.65 eV and degrades as $(eKE)^{3/2}$ at higher electron kinetic energies.

The experiments described below were performed with the third and fourth harmonic frequencies (355 nm, 3.49 eV and 266 nm, 4.66 eV, respectively) of a Nd:YAG laser. The plane-polarized laser beam can be rotated using a half-wave plate. In the spectra shown, unless otherwise specified, the laser beam is polarized at $\theta = 54.7°$ (magic angle)[30] with respect to the direction of electron collection. The spectra presented here are averaged for 100 000–500 000 laser shots at 20 Hz repetition rate, and smoothed by convolution with a 5 meV full-width at half-maximum (FWHM) Gaussian. In order to account for the small background electron signal which results from scattered light interacting with the photodetachment chamber surfaces in the 4.66 eV spectra, a background spectrum is collected, smoothed and subtracted from the data.

III. RESULTS

The photoelectron spectra of the odd-numbered carbon anions, C_{2n+1}^- ($n = 1$–4), obtained using a photon energy of 4.66 eV, are presented in Fig. 1. In these and all other photoelectron spectra, the eKE is related to the internal energy of the neutral molecule by the expression,

$$eKE = h\nu - EA - T_0 + T_0^- - E_v^0 + E_v^-. \quad (1)$$

Here, $h\nu$ is the laser photon energy, EA is the electron affinity of the neutral species, T_0^0 and T_0^- are the term values of the specific neutral and anion electronic states, respectively. E_v^0 and E_v^- are the vibrational energies (above the zero point energy) of the neutral and anion, respectively. Rotational contributions to molecular internal energy are neglected. As indicated by Eq. (1), the peaks occurring at low-

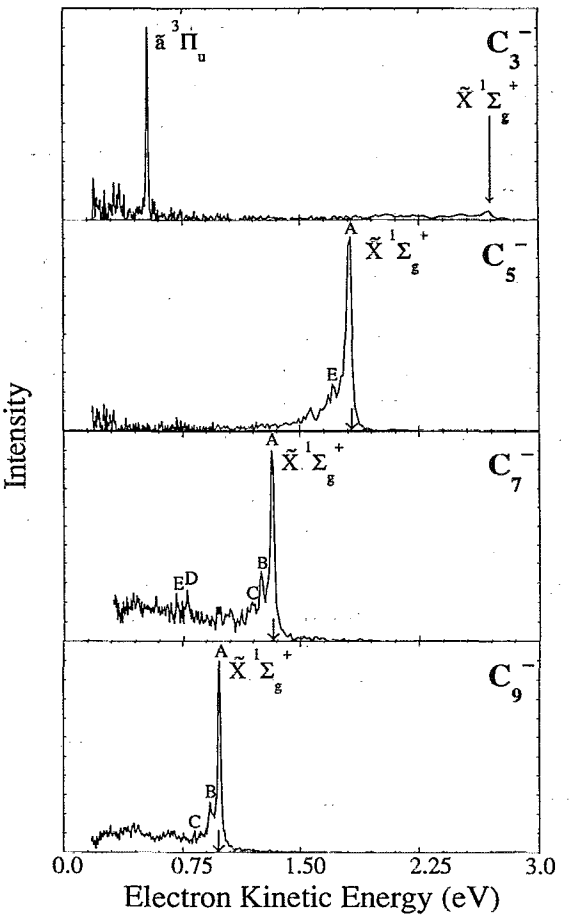

FIG. 1. Photoelectron spectra of C_3^-, C_5^-, C_7^-, and C_9^- at 266 nm (4.66 eV). Arrows indicate electron affinity of linear carbon chain.

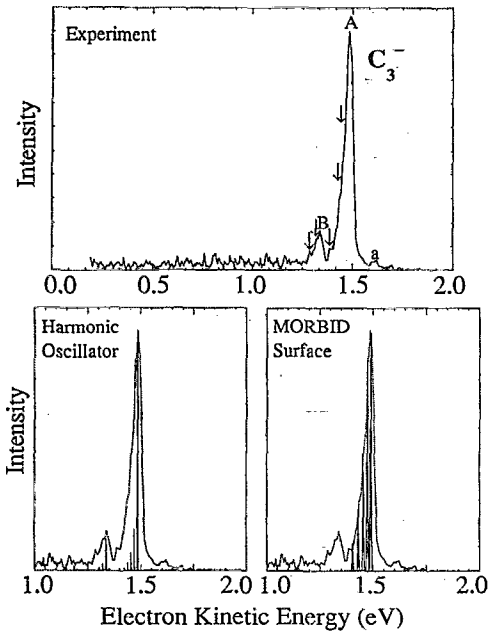

FIG. 2. (top) Photoelectron spectrum of C_3^- at 355 nm (3.49 eV) (top); (bottom) simulations of C_3^- photoelectron spectrum at 355 nm using a separable harmonic oscillator approximation and a ($\nu_2 \times \nu_2$) cross section of MORBID potential energy surface. Both simulations are performed at 0.002 eV resolution to illustrate effect of anharmonicity upon ν_2 bend mode progression intensities.

est eKE in the photoelectron spectrum correspond to the highest internal energy states of the neutral.

As n increases for the C_{2n+1} molecules, the spectral features shift to lower eKE, indicating an increase in electron affinity. In the C_3^- spectrum, there are poorly resolved features at high eKE which correspond to the ground state of C_3. However, there is a single well-resolved peak at low eKE which corresponds to an excited electronic state of C_3. In each of the spectra of C_5^-, C_7^-, and C_9^-, there is a short, congested progression extending to lower eKE.

Since our experimental resolution degrades at higher eKE, experiments using a lower photon energy (3.49 eV) yield better resolved spectra of the ground state progressions of C_3 and C_5 (Figs. 2 and 3). The C_3^- spectrum contains two peaks which have multiple shoulders. The peaks and shoulders are indicated with letters and arrows, respectively. The higher resolution spectrum of C_5^- contains many small peaks in addition to the large peak A, indicating that vibrational excitation of C_5 occurs upon photodetachment of the C_5^- anion. Peak positions and assignments for the C_5^-, C_7^-, and C_9^- spectra, discussed in more detail below, are summarized in Table I.

The photoelectron spectra obtained at 4.66 eV for the even carbon anions, C_{2n}^- ($n = 1$–4), are shown in Fig. 4. As was the case for the C_{2n+1}^- spectra, the C_{2n}^- spectra strongly resemble each other, but the electron affinities of the even-numbered species are higher than their neighboring C_{2n+1} counterparts. In the C_2^- and C_4^- spectra, there are several peaks extending over a larger energy range than the progressions of the C_{2n+1}^- spectra, with a somewhat irregular intensity pattern. Only limited portions of the C_6^- and C_8^- spectra are obtainable with the 4.66 eV photon energy due to the high EAs of C_6 and C_8. The peak positions and assignments for the C_2^- spectrum are in Table II, and those for the C_4^- and C_6^- spectra are listed Table III.

Photoelectron spectra of C_{10}^- and C_{11}^-, taken with a 4.66 eV photodetachment energy, are displayed in Fig. 5. These two spectra have a significantly different appearance than the spectra of C_2^-–C_9^-. The C_{10}^- spectrum (Fig. 5) contains broad unresolved band structure possibly indicative of transitions involving multiple electronic states. However, in the C_{11}^- spectrum, there are resolved peaks superimposed on a broad spectrum which resembles the C_{10}^- spectrum. A long low-intensity tail extends to the high eKE regions of both spectra. These long tails also appear in the C_6^- and C_8^- spectra and with significantly less intensity in the C_5^- spectrum. This is discussed further in Sec. IV D.

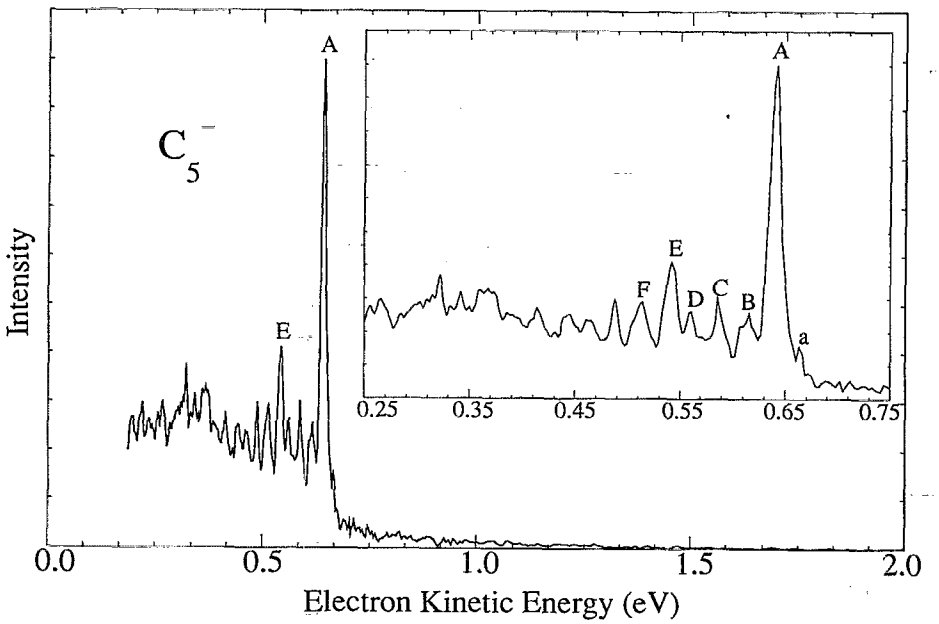

FIG. 3. Photoelectron spectrum of C_5^- at 355 nm. The inset shows an expanded spectrum including labels discussed in text.

TABLE I. Peak positions and assignments for the C_5^-, C_7^-, and C_9^- photoelectron spectra.

Molecule	Peak	Position	Splitting from origin (cm^{-1})	Assignment
C_5[a]	A	0.641	0	Origin
	B	0.616	202	7_0^2
	C	0.586	444	5_0^2
	D	0.560	653	$5_0^2 7_0^2$
	E	0.542	798	2_0^1
	F	0.514	1024	6_0^2
C_7[b]	A	1.302	0	Origin
	B	1.234	548	3_0^1
	C	1.179	992	7_0^2
	D	0.773	4267	4_0^2
C_9[c]	A	0.978	0	Origin
	B	0.918	484	4_0^1
	C	0.822	1258	3_0^1

[a] The ν_2 mode is a symmetric stretch and the ν_5, ν_6, and ν_7 modes are bending modes [see Fig. 8(b)].
[b] The ν_3 mode is a symmetric stretch, ν_4 is an antisymmetric stretch, and ν_7 is a bending mode.
[c] The ν_3 and ν_4 modes are symmetric stretches.

TABLE II. Peak positions and assignments for the C_2^- photoelectron spectrum.

Peak	Position	Assignment[a] ($C_2 \leftarrow C_2^-$)
A	1.384	$X\,^1\Sigma_g^+ (v'=0) \leftarrow X\,^2\Sigma_g^+ (v''=0)$
B	1.310	$a\,^3\Pi_u (v'=0) \leftarrow X\,^2\Sigma_g^+ (v''=0)$
C	1.153	$X\,^1\Sigma_g^+ (v'=1) \leftarrow X\,^2\Sigma_g^+ (v''=0)$
D	1.111	$a\,^3\Pi_u (v'=1) \leftarrow X\,^2\Sigma_g^+ (v''=0)$
E	0.849	$A\,^1\Pi_u (v'=0) \leftarrow A\,^2\Pi_u (v''=0)$
F	0.362	$A\,^1\Pi_u (v'=0) \leftarrow X\,^2\Sigma_g^+ (v''=0)$
a	1.542	$a\,^3\Pi_u (v'=0) \leftarrow X\,^2\Sigma_g^+ (v''=1)$
b	1.609	$X\,^1\Sigma_g^+ (v'=0) \leftarrow X\,^2\Sigma_g^+ (v''=1)$
c	1.804	$a\,^3\Pi_u (v'=0) \leftarrow A\,^2\Pi_u (v''=0)$

[a] For each peak assigned, there are also underlying sequence bands which are unresolved in the spectrum.

Data collected for C_4^- at two different laser polarizations are shown in Fig. 6. The important difference between the two spectra is the variation of the relative intensities of peaks B and D as a function of laser polarization angle; these peaks are essentially absent in the $\theta = 90°$ spectrum. This behavior will be addressed in greater detail below.

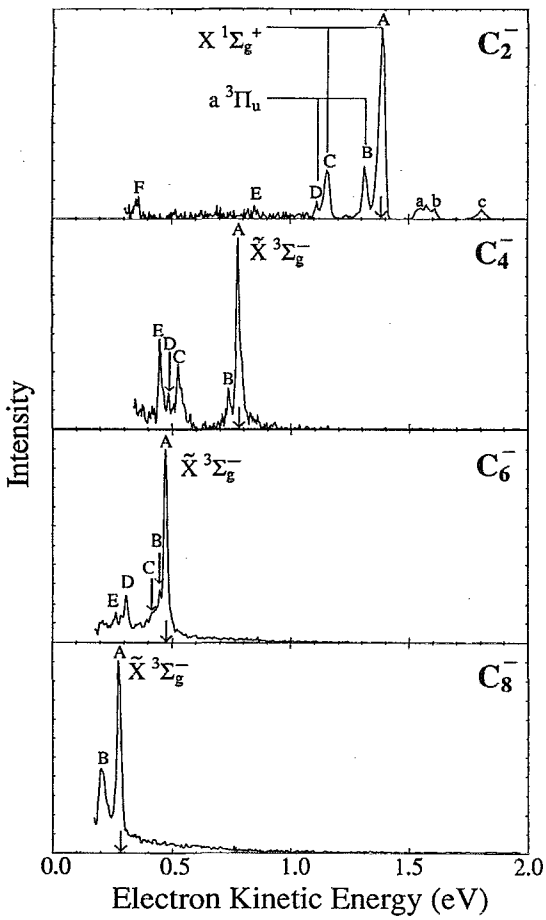

FIG. 4. Photoelectron spectra of C_2^-, C_4^-, C_6^-, and C_8^- at 266 nm. Arrows on axis indicate electron affinity of linear carbon chain.

IV. ANALYSIS AND DISCUSSION

In this section, the C_2^- and C_3^- photoelectron spectra are analyzed in considerable detail and used to lay the framework for the discussion of the larger carbon molecules. The spectroscopy of C_2 (Refs. 31 and 32) and C_3 (Refs. 9 and 33) has been studied intensely for several years using a variety of techniques, including anion photoelectron spectroscopy.[18,34,35] Therefore, the discussion of these systems will be limited to the new information provided by the photoelectron spectra presented here. The spectra of the larger molecules are treated more qualitatively.

TABLE III. Peak positions and assignments for the C_4^- and C_6^- photoelectron spectra.

Molecule	Peak	Position	Splitting from origin (cm^{-1})	Assignment
C_4[a]	A	0.778	0	Origin
	B	0.736	339	4_0^1
	C	0.526	2032	1_0^1
	D	0.487	2347	$1_0^1 4_0^1$
	E	0.451	2637	$^1\Delta_g$[b]
C_6[c]	A	0.475	0	Origin
	B	0.451	194	Sequence band
	C	0.416	480	3_0^1 or 7_0^2
	D	0.312	1315	2_0^1
	E	0.269	1660	Sequence band

[a] The ν_1 mode is a symmetric stretch and ν_4 is a bend mode [see Fig. 8(a)].
[b] Peak E is assigned to an excited electronic state, see text.
[c] Both ν_2 and ν_3 are symmetric stretches while ν_7 is a bend mode.

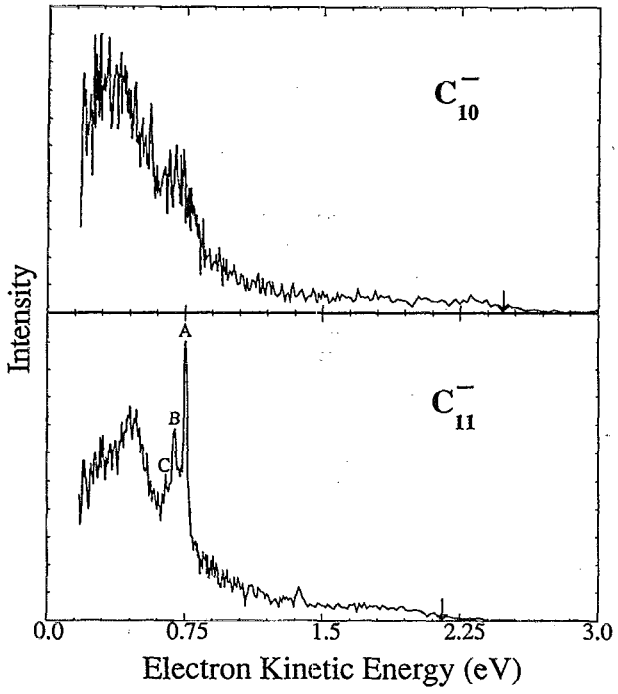

FIG. 5. Photoelectron spectra of C_{10}^- and C_{11}^- at 266 nm. Arrows indicate estimated electron affinity for monocyclic isomer.

The analyses for all the spectra presented here are done within the Franck–Condon approximation. The transition intensity, I, for the process,

$$C_n^-(v'') \rightarrow C_n(v') + e^- \tag{2}$$

is governed by the expression,

$$I \propto |\tau_e|^2 |\langle \Psi_{v''} | \Psi_{v'} \rangle|^2. \tag{3}$$

Here τ_e is the electronic transition dipole moment and the Franck–Condon factor, $|\langle \Psi_{v''} | \Psi_{v'} \rangle|^2$, depends upon the spatial overlap of the vibrational wave functions of the anion and the neutral.[36] In this approximation, it is assumed that τ_e does not change significantly over the spatial range covered by the nuclear wave function and is treated as a constant in the spectral simulations.

A. C_2

Diatomic carbon, C_2, has been thoroughly investigated using both absorption and emission spectroscopy.[37] C_2^-, one of the few anions known to possess bound excited electronic states,[38] has also been well characterized.[39] Recently, Ervin and Lineberger have obtained a vibrationally resolved photoelectron spectrum of the C_2^- anion.[35] The use of a higher photodetachment energy (4.66 eV) in the experiments described here reveals transitions to excited vibrational levels and an excited electronic state of C_2 which could not be seen by Ervin and Lineberger.

Shown in Fig. 7 is the C_2^- photoelectron spectrum obtained at 4.66 eV photodetachment energy. The spectrum has been simulated (Fig. 7, bottom) using molecular constants obtained from high resolution data[32] by varying the vibrational temperature, electron affinity, and relative intensities of different electronic transitions. Both C_2 and C_2^- have low-lying excited electronic states. As a result, several

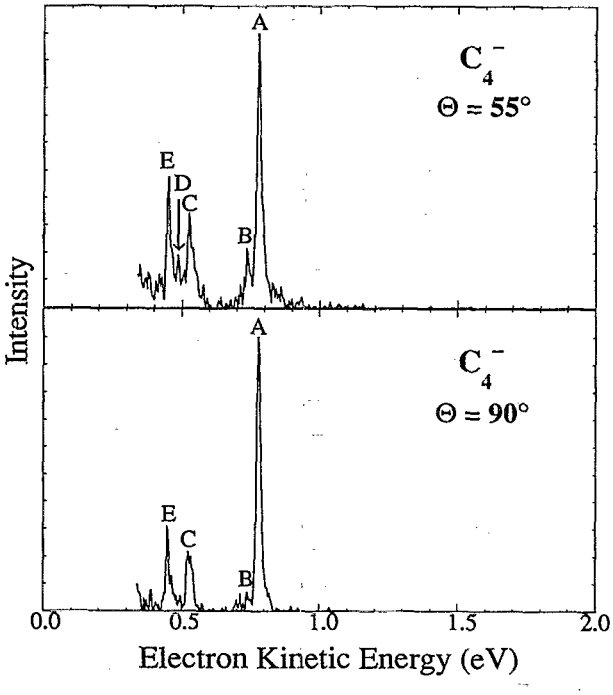

FIG. 6. Photoelectron spectra of C_4^- at 266 nm showing laser polarization dependence of peaks B and D. Laser polarization angles are $\theta = 55°$ and 90° with respect to direction of electron collection.

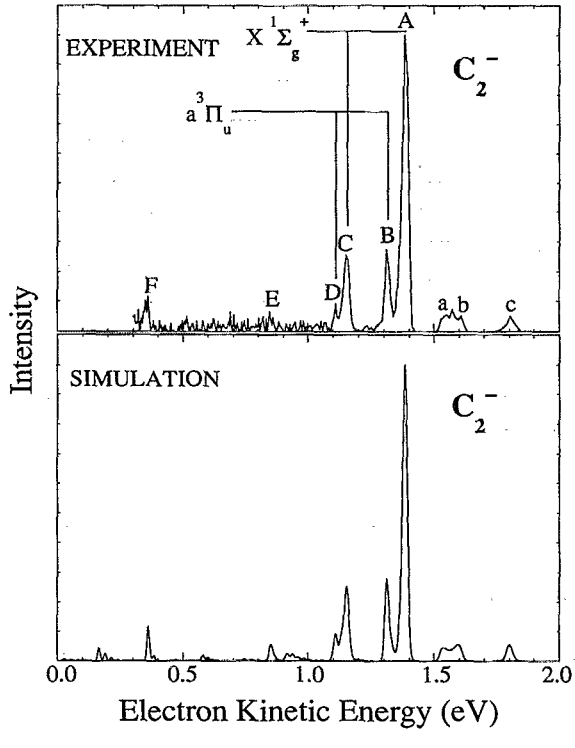

FIG. 7. Photoelectron spectrum of C_2^- at 266 nm and best-fit Franck–Condon simulation using EA, temperature, and relative electronic dipole transition moments as variables.

photodetachment transitions are energetically accessible using the 4.66 eV detachment photon energy. Some peak assignments are indicated in Fig. 7 and details are given in Table II. One-electron photodetachment of $C_2^- X\,^2\Sigma_g^+$ $(...2\sigma_u^2 1\pi_u^4 3\sigma_g^1)$ can produce the $C_2 X\,^1\Sigma_g^+$ $(...2\sigma_u^2 1\pi_u^4)$, $a\,^3\Pi_u$ and $A\,^1\Pi_u$ states $(...2\sigma_u^2 1\pi_u^3 3\sigma_g^1$ for the latter excited states, $T_e = 0.089$ and 1.040 eV, respectively).[32] Peaks A and B in Fig. 7 are the origins of the $C_2 X\,^1\Sigma_g^+ \leftarrow C_2^- X\,^2\Sigma_g^+$ and $C_2 a\,^3\Pi_u \leftarrow C_2^- X\,^2\Sigma_g^+$ transitions, respectively. The $C_2 X\,^1\Sigma_g^+ (v' = 1) \leftarrow C_2^- X\,^2\Sigma_g^+ (v'' = 0)$ and $C_2 a\,^3\Pi_u (v' = 1) \leftarrow C_2^- X\,^2\Sigma_g^+ (v'' = 0)$ transitions, which were near the cutoff region for the energy analyzer of the Lineberger experiment,[35] are clearly defined in Fig. 7 (peaks C and D, respectively). At even lower eKE, peak F represents the origin of the $C_2 A\,^1\Pi_u \leftarrow C_2^- X\,^2\Sigma_g^+$ transition. From peak A, we obtain a value of 3.273 ± 0.008 eV for the electron affinity of C_2. This agrees well with the value of 3.269 ± 0.006 eV recently measured by Ervin and Lineberger.[35,40]

It is apparent in the C_2^- spectrum that peaks corresponding to π-electron photodetachment from the $C_2^- X\,^2\Sigma_g^+$ state (peaks B, D, and F) are consistently less intense than the those representing σ-electron photodetachment from the same electronic state of C_2^- (peaks A and C). This pattern suggests that the photodetachment cross section for removal of a 3σ electron from this state is higher than that for removal of a 1π electron from the $C_2^- X\,^2\Sigma_g^+$ state.

As in Lineberger's spectrum, the $C_2 X\,^1\Sigma_g^+ (v' = 0) \leftarrow C_2^- X\,^2\Sigma_g^+ (v'' = 1)$ and $C_2 a\,^3\Pi_u (v' = 0) \leftarrow C_2^- X\,^2\Sigma_g^+ (v'' = 1)$ "hot" band transitions occur (labeled as a and b, respectively). While the vibrational distribution of the ions produced in our laser vaporization source could be controlled to a considerable extent for the other carbon anions, C_2^- could only be generated under conditions that produced anions with considerable vibrational excitation. The best fit to the spectrum was obtained assuming a vibrational temperature of 3000 K. In addition to the "hot bands," the anion vibrational excitation gives rise to many sequence bands under the $v' = 0$ and the $v' = 1$ peaks of the progressions in the $X\,^1\Sigma_g^+$ and the $a\,^3\Pi_u$ states of C_2.

The spectrum also shows photodetachment transitions from the low-lying $C_2^- A\,^2\Pi_u$ first excited state. Signal resulting from the photodetachment of this anion state is observed because its lifetime ($\tau_{rad} \approx 50\,\mu s$)[41] is comparable to the amount of time between anion formation and photodetachment. One-electron transitions can occur from $C_2^- A\,^2\Pi_u$ $(...2\sigma_u^2 1\pi_u^3 3\sigma_g^2$, $T_e = 0.494$ eV)[39] to C_2 in the $a\,^3\Pi_u$, $b\,^3\Sigma_g^-$ $(...2\sigma_u^2 1\pi_u^2 3\sigma_g^2$, $T_e = 0.798$ eV)[31] and $A\,^1\Pi_u$ excited states. Peak c in the spectrum is assigned to the origin of the $C_2 a\,^3\Pi_u \leftarrow C_2^- A\,^2\Pi_u$ transition. Label E in the spectrum represents the energy at which signal is expected for the $C_2 A\,^1\Pi_u \leftarrow C_2^- A\,^2\Pi_u$ transition; a very small peak may be present there in the experimental spectrum. Electrons resulting from the $C_2 b\,^3\Sigma_g^- \leftarrow C_2^- A\,^2\Pi_u$ transition are expected to appear at eKE ≈ 1.1 eV, close to peak D. However, there does not appear to be a significant contribution to the spectrum from this transition.

B. C_3

C_3 has been shown to be a linear but floppy molecule. The C_3^- anion is predicted to be linear[42] with a $^2\Pi_g$ $(...4\sigma_g^2 3\sigma_u^2 1\pi_u^4 1\pi_g^1)$ ground state which is considerably more rigid than C_3 due to the partly filled π_g orbital. The 4.66 eV photoelectron spectrum of C_3^- (Fig. 1) shows transitions to the two electronic states of C_3 which are energetically accessible via one-electron photodetachment of C_3^-. While photodetachment of the $1\pi_g$-electron leaves C_3 in its $\tilde{X}\,^1\Sigma_g^+$ ground state $(...4\sigma_g^2 3\sigma_u^2 1\pi_u^4)$, removal of the $3\sigma_u$-electron produces the $C_3 \tilde{a}\,^3\Pi_u$ first excited state $(...4\sigma_g^2 3\sigma_u^1 1\pi_u^4 1\pi_g^1)$. The spectrum of C_3^- obtained with a photodetachment energy of 3.49 eV (Fig. 2) reveals vibrational details of the $C_3 \tilde{X}\,^1\Sigma_g^+$ ground state.

Understanding the features of this spectrum requires consideration of the Franck–Condon principle for molecules with more than one vibrational mode. For an anion and neutral belonging to the same symmetry point group, transitions can occur from the anion ground state to any quantum state of a totally symmetric vibrational mode (e.g., ν_1 for C_3). Excitation of these modes occurs primarily when there is a difference in bond lengths between the anion and neutral. Typically, excitation occurs in those vibrational modes which most strongly resemble the change in geometry upon anion photodetachment. For nontotally symmetric vibrational modes (e.g., ν_2 and ν_3 for C_3), symmetry forbids transitions from the anion ground state to odd quanta of excitation in the neutral. From the anion ground state, only transitions to even quanta of these neutral vibrational modes will be observed, and transitions to states with $v > 0$ only occur when there is a large difference in vibrational frequency between the anion and the neutral. For example, little excitation is expected in the antisymmetric stretch of C_3 since the ν_3 frequencies are predicted[42] to be comparable for C_3 and C_3^-.

In the 3.49 eV photoelectron spectrum of C_3^- (Fig. 2), peaks A and B are assigned to the 0–0 and the 1_0^1 members of the $C_3 \tilde{X}\,^1\Sigma_g^+ \leftarrow C_3^- \tilde{X}\,^2\Sigma_g^+$ transition, respectively. Our peak spacing of 1200 ± 100 cm^{-1} for the neutral symmetric stretch agrees well with the value of 1224.5 cm^{-1} from higher resolution studies.[43,44,45] The dominance of peak A indicates a fairly small bond length difference between C_3^- and C_3, in agreement with the *ab initio* results.[42] Peak a is a hot band assigned to the 1_1^0 transition, providing a frequency for the C_3^- ν_1 symmetric stretch of 1075 ± 100 cm^{-1}, in good agreement with *ab initio* results (1175 cm^{-1}).[42] The intensity of peak a indicates that the anion vibrational temperature is < 450 K.

Peaks A and B are considerably broader (≈ 0.15 eV) than the experimental resolution (≈ 0.025 eV). This breadth is due to underlying vibrational structure which appears as a series of poorly resolved shoulders (indicated by arrows). Lineberger and co-workers partially resolve these transitions in their higher resolution C_3^- photoelectron spectrum.[46] These shoulders result from two types of transitions. The first type, which provides most of the intensity for the

shoulders, is the 2_0^{2n} progression in the C_3 bend. The second type is the 1_n^n sequence band progression resulting from the 149 cm^{-1} frequency difference for ν_1 between C_3 and C_3^-.

The C_3 bending mode has a fundamental frequency[9,47] of 63 cm^{-1}, which is significantly different from the calculated anion bending frequency ($\nu_2 \approx 300$ cm^{-1}).[42] In addition, the neutral bending mode is very anharmonic and couples to both of the other C_3 vibrational modes.[45] All of these effects can produce excitation of the neutral upon anion photodetachment, and the latter two effects create a vibrational pattern for C_3 which is poorly described by a separable normal mode approximation.[9,45,48]

The inadequacy of the normal mode approximation for describing the C_3 bend can been seen in Fig. 2. This shows the results of a Franck–Condon calculation assuming separable harmonic oscillators for the ν_1 symmetric stretch and the ν_2 degenerate bend. The anion wave function is generated assuming an anion bending frequency of 300 cm^{-1} based upon *ab initio* predictions,[42,49] and a symmetric stretch frequency of 1075 cm^{-1} (discussed below). The simulation shows some excitation of the neutral bend due to the large difference between the C_3 and C_3^- bend frequencies. However, the frequency difference alone does not yield sufficient bend excitation in C_3.

In order to account for this discrepancy, an exact quantum mechanical calculation[50] of eigenvalues and Franck–Condon intensities (Fig. 2), was performed on a two-dimensional cross section ($\nu_2 \times \nu_2$) of the semiempirical Morse oscillator rigid bender internal dynamics (MORBID)[51] potential energy surface.[52] This potential energy surface, generated by fitting Rohlfing's laser-induced fluorescence data,[45] includes the anharmonicity and vibrational coupling present between all three vibrational modes. The anion wave function is the same as that used in the harmonic oscillator simulation. Since the calculation considers *only* the bend mode, the changes in the simulation from the harmonic oscillator results are due to anharmonicity along the C_3 ν_2 coordinate. It is clear from this simulation that the extreme anharmonicity of the bend mode drastically changes the intensities of the 2_0^{2n} transitions. Although the experimental spectra do not resolve all this structure, the simulations demonstrate qualitatively that the excitation of the bending mode is due to two effects: the change in frequency of the bending mode upon photodetachment and, more importantly, the floppiness, or anharmonicity, of the C_3 bend mode.

Removal of the σ_u-electron from the C_3^- anion leaves the neutral with the $...4\sigma_g^2 3\sigma_u^1 1\pi_u^4 1\pi_g^1$ electronic configuration corresponding to either the C_3 $\tilde{a}\,^3\Pi_u$ or $\tilde{A}\,^1\Pi_u$ states. Peak B in the 4.66 eV photoelectron spectrum of C_3^- (Fig. 1), is assigned to the 0–0 transition to the $\tilde{a}\,^3\Pi_u$ first excited state placing it 2.118 ± 0.026 eV above the ground state. While the $\tilde{a}\,^3\Pi_u$ state has been observed in matrix emission experiments due to an intersystem crossing from the $\tilde{A}\,^1\Pi_u$ state,[44,53] the term value for C_3 $\tilde{a}\,^3\Pi_u$ had not previously been directly measured in the gas phase because the $\tilde{a}\,^3\Pi_u \leftarrow \tilde{X}\,^1\Sigma_g^+$ transition is optically spin-forbidden. Our T_0 for the $\tilde{a}\,^3\Pi_u$ state agrees well with matrix values obtained by Weltner and McLeod[44] (2.117 eV in Ne, 2.100 eV in Ar) and Bondybey and English[53] (2.117 eV in Ne) and the calculations of Perić–Radić *et al.* (2.04 eV).[54] The dominance of the 0–0 transition for the $\tilde{a}\,^3\Pi_u$ state indicates a very small difference in geometry between C_3^- and the first excited state of C_3. This agrees with geometry calculations for C_3 and C_3^-,[42,54] as well as intuition, because the detached electron originates from the effectively nonbonding C_3^- σ_u-orbital. The r_0 bond length for the $\tilde{a}\,^3\Pi_u$ state is 1.298 Å.[9(b)]

C. C_4 through C_9

The photoelectron spectra of C_4^-–C_9^- show many similarities. Each is dominated by a sharp peak (labeled A in each spectrum) and contains several smaller peaks at lower eKE. Peak A is assigned to the $C_n(v'=0) \leftarrow C_n^-(v''=0)$ transition in each spectrum. As in C_3, the dominance of this transition indicates only a small change in geometry upon photodetachment. As discussed earlier, there is experimen-

TABLE IV. Calculated and experimental frequencies for C_5 (cm^{-1}).

Reference	Calculation	ν_1 (σ_g)	ν_2 (σ_g)	ν_3 (σ_u)	ν_4 (σ_u)	ν_5 (π_g)	ν_6 (π_u)	ν_7 (π_u)
Botschwina[a]	CEPA-1	2008	792	2169	1478	209	570	119
Kurtz[b]	MBPT(2)/6-31G*	2018	786	2358	1471	281	480	131
Gijbels[c]	MP2/6-31G*	1877	731	2193	1368	261	453	121
Raghavachari[d]	HF/6-31G*	1998	768	2110	1469	200	583	101
	Experiment							
Weltner[e]	IR matrix	(1904)[f]	(785)[f]	2164	···	···	···	···
Amano[g]	IR gas-phase	···	···	2169	···	218	···	118
Saykally[h]	IR gas-phase	···	···	2169	···	···	···	···
Present work	UV-PES	···	798	···	···	222	512	101

[a] P. Botschwina and P. Sebald, Chem. Phys. Lett. **160**, 485 (1989).
[b] Reference 58(a).
[c] Reference 58(c); scaled by 0.93.
[d] Reference 13; scaled by 0.89.
[e] Reference 22.
[f] Predicted by force constant analysis.
[g] Reference 10(b) and (c).
[h] Reference 10(a).

TABLE V. Electron affinities for linear carbon molecules.

Molecule	Electron affinity (eV)[a]		*Ab initio* Results (eV)
	Present work	Other	
C_2	3.273 (0.008)	3.269 (0.006)[b]	3.112[e]
		3.30 (0.1)[c]	3.43[f]
C_3	1.995 (0.025)	1.981 (0.020)[d]	2.0[g,h]
		1.95 (0.1)[c]	1.58[i]
C_4	3.882 (0.010)	3.7 (0.1)[c]	3.39[j]
			3.41[i]
C_5	2.839 (0.008)	2.8 (0.1)[c]	2.43[i]
C_6	4.185 (0.006)	4.1 (0.1)[c]	3.69[i]
C_7	3.358 (0.014)	3.1 (0.1)[c]	···
C_8	4.379 (0.006)	4.42 (0.1)[c]	···
C_9	3.684 (0.010)	3.70 (0.1)[c]	···
C_{10}	···	···	···
C_{11}	3.913 (0.008)	4.0 (0.1)[c]	···

[a] Uncertainties given in parentheses.
[b] Reference 35.
[c] Reference 18.
[d] Reference 34.
[e] J. A. Nichols and J. Simons, J. Chem. Phys. **86**, 6972 (1987).
[f] M. Zeitz, S. D. Peyerimhoff, and R. J. Buenker, Chem. Phys. Lett. **64**, 243 (1979).
[g] Reference 42.
[h] K. K. Sunil, A. Orendt, and K. D. Jordan, Chem. Phys. **89**, 245 (1984).
[i] Reference 56.
[j] Reference 64.

tal and theoretical evidence for the existence of linear neutral carbon molecules with up to nine atoms. In addition, *ab initio* calculations predict linear ground state structures for all C_n^- ($n \leqslant 6$) anions.[55] Based upon the appearance of our spectra and these other results, the peaks in the C_4^-–C_9^- spectra are assigned to transitions between the linear forms of the anion and the neutral. The electron affinities for the linear carbon molecules are then determined from the position of peak A in each spectrum. The observed EAs for linear C_2–C_9 (and C_{11}) are compiled in Table V. Contributions from sequence bands, uneven rotational contours, or spin-orbit splittings have not been assessed and so the EA may deviate slightly from the value presented. These effects are the basis for the error bars reported. The uncertainties vary as a function of the eKE at the origin of the spectrum. Also listed for comparison are the EAs obtained from other experiments and from *ab initio* calculations. The EAs of the even molecules are consistently higher than their neighboring odd-numbered counterparts. In general, the EAs agree with the values obtained by Yang *et al.*[18] at significantly lower resolution and confirm the even–odd alternation of ground state symmetries for small carbon molecules. The EAs calculated by Adamowicz[56] appear to be consistently low by $\approx$0.5 eV for the C_{2n} molecules and by $\approx$0.4 eV for the C_{2n+1} molecules.

Most of the smaller peaks in the spectra presented here can be assigned to either vibrational progressions of the neutral or "hot bands." As discussed above, in photoelectron spectroscopy, excitation is seen principally in totally symmetric vibrational modes upon photodetachment. The combination of this principle and *ab initio* calculations of vibrational frequencies provides much of the basis for the assignments presented.

In addition to the vibrational progression assignments, some of the smaller peaks are assigned to excited electronic states of the linear neutral molecules (see discussion of C_4, C_6, and C_8). In the spectra of C_6^-, C_8^-, and C_5^- (3.49 eV spectrum only)[57] there are long tails extending to high eKE, which are assigned to transitions involving nonlinear carbon neutrals and/or anions. The analysis of the linear C_n^- ($n \leqslant 9$) is divided into two sections: one for molecules with an odd-number of carbon atoms (C_{2n+1}) and the other for those with an even-number of carbon atoms (C_{2n}). The linear C_{2n+1} molecules are all closed-shell, $^1\Sigma_g^+$, species while the linear C_{2n} molecules all have open-shell $^3\Sigma_g^-$ ground states.

1. C_5, C_7, and C_9

The photoelectron spectrum of C_5^- recorded with a photon energy of 4.66 eV (Fig. 1), shows a short vibrational progression of the neutral. At higher resolution (3.49 eV, Fig. 3), it is evident that several modes, including symmetric stretch and nontotally symmetric bend modes, are excited upon photodetachment of the anion. The forms of these vibrational modes are shown in Fig. 8(b). The assignments of the peaks in the C_5 spectra (Table I) are based upon *ab initio* results.[13,58] Peaks B, C, and F are assigned to the 7_0^2, 5_0^2, and 6_0^2 transitions, respectively. The bend frequencies obtained from these assignments are $2\nu_5/2 = 222$ cm^{-1} and $2\nu_7/2 = 101$ cm^{-1}, in agreement with the tentative assignments proposed by Moazzen-Ahmadi *et al.*,[10] and $2\nu_6/2 = 512$ cm^{-1}. The uncertainty in these values is $\sim$45 cm^{-1}. Peak D corresponds to the $5_0^2 7_0^2$ combination band.

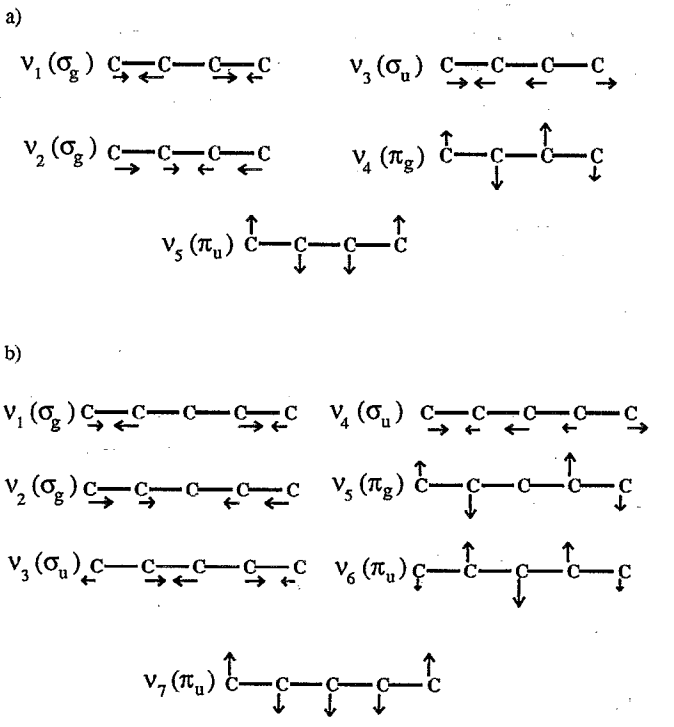

FIG. 8. Forms of normal modes for (a) C_4 and (b) C_5.

Peak E is assigned to the 2_0^1 transition providing a symmetric stretch frequency of $\nu_2 = 798 \pm 45\ cm^{-1}$. Vala *et al.*,[22] using force constants obtained from their ν_3 measurement in the matrix environment, predict frequencies of 1904 and 785 cm^{-1} for the ν_1 and ν_2 symmetric stretch modes. Our value for ν_2 agrees well with their prediction. The *ab initio* and experimental frequencies for C_5 are compiled in Table IV.

In addition to these assigned peaks, there are several other peaks to low eKE which do not appear in the 4.66 eV spectrum due to the lower resolution there. Although some of these peaks could potentially be assigned to C_5 vibrations based upon agreement with *ab initio* results, higher resolution (10 cm^{-1}) threshold photodetachment results obtained in this laboratory indicate that these peaks may actually be due to transitions involving another electronic state of C_5.[59] This assignment is supported by a comparison of the two C_5^- spectra presented here. The peaks to low eKE are *relatively* more intense in the 3.49 eV spectrum than in the 4.66 eV spectrum. It is well-documented that the partial cross sections for different photoionization transitions have different energy dependencies.[60] It appears that the partial photodetachment cross section for the transition to the excited state of C_5 decreases relative to the $X\,^1\Sigma_g^+ \leftarrow X\,^2\Sigma_g^+$ transition with increasing photodetachment energy. In agreement with this observation, there was little or no signal observed for this transition in the C_5^- photoelectron spectrum obtained by Yang *et al.*[18] using a photodetachment energy of 7.9 eV.

The photoelectron spectrum of C_7^- obtained with a photon energy of 4.66 eV (Fig. 1) is similar to that of C_5^-. Resolution limitations at higher eKE combined with additional low frequency bending vibrations of C_7 result in fewer fully resolved vibrational features, but some of the peaks can be assigned (Table I) using *ab initio* results for the vibrational frequencies.[58] Peak B is assigned to the 3_0^1 transition, providing a symmetric stretch vibrational frequency of $\nu_3 = 548 \pm 90\ cm^{-1}$. As in C_5^-, bending modes are excited upon photodetachment of C_7^-. Peak C, tentatively assigned to the 7_0^2 transition, gives the bend frequency of $\nu_7 = 496 \pm 110\ cm^{-1}$. The spacing of peak D from the origin agrees well with twice the value obtained for the ν_4 antisymmetric stretch mode by Heath and Saykally.[11] However, as in C_5, peaks D and E (and structure to lower eKE) may result from transitions involving an excited electronic state of the neutral.

While the C_9^- spectrum (Fig. 1) resembles the spectra of C_5^- and C_7^-, it primarily shows two symmetric stretch vibrational progressions. Peaks B and C are assigned to the 4_0^1 and 3_0^1 transitions providing symmetric stretch frequencies of $\nu_3 = 1258 \pm 50\ cm^{-1}$ and $\nu_4 = 484 \pm 48\ cm^{-1}$.

All of the odd-numbered molecules discussed thus far show excitation in the breathing-type symmetric stretch [e.g., ν_2 for C_5, Fig. 8(b)], which is the lowest frequency symmetric stretch in all cases. This suggests that all the C–C bonds for these systems change in the same manner upon photodetachment, whether it be to lengthen or shorten. The *ab initio* results for the C_3/C_3^- (Ref. 42) and C_5/C_5^- (Ref. 61) systems indicate that all the neutral bond lengths are shorter than those of the ions, in agreement with these results. In addition, as the chain grows in length, the frequency of this mode decreases: $\nu_1(C_3) = 1200\ cm^{-1}$; $\nu_2(C_5) = 798\ cm^{-1}$; $\nu_3(C_7) = 548\ cm^{-1}$; and $\nu_4(C_9) = 484\ cm^{-1}$. Since the electronic structure is expected to be very similar for these molecules, one might expect comparable force constants for similar types of vibrational modes. As a result, the decrease in frequency as a function of chain length results mainly from the increase in reduced mass of the longer chains.

2. C_4, C_6, and C_8

The 4.66 eV photoelectron spectrum of C_4^- shown in Fig. 4 has four resolved peaks to the low eKE side of the origin. Theoretical calculations for C_4 predict two nearly isoenergetic isomers which have been considered for the ground state: a $^3\Sigma_g^-$ $D_{\infty h}$ linear structure and a ^1A_g D_{2h} rhombic structure. At the highest levels of theory, the two are separated by as little as 1 kcal/mol.[62,63] The electron affinity of C_4 determined from the C_4^- spectra, 3.882 ± 0.010 eV, agrees reasonably well with Yang *et al.*'s value of 3.7 ± 0.1 eV. From their CEI results, Algranati *et al.*[26] report an electron affinity of the rhombic isomer of C_4 as 2.1 ± 0.1 eV. Comparison with Watts *et al.*'s calculated EA for C_4 of 3.39 eV (Ref. 64) and Adamowicz's[56] EAs for the linear and rhombic isomers of C_4 (3.45 and 2.03 eV, respectively) further supports the assignment of the C_4^- photoelectron spectral features to a linear anion→linear neutral photodetachment process.

Peak C is assigned to the 1_0^1 transition, providing a symmetric stretch vibrational frequency of $\nu_1 = 2032 \pm 50\ cm^{-1}$ (*ab initio* value[58] for $\nu_1 = 2150\ cm^{-1}$). According to recent geometry calculations for linear C_4 and C_4^- at the SDQ-MBPT(4) level of theory,[64] upon photodetachment of C_4^- the outer bonds will shorten while the inner bond will stretch. The strong resemblance of this geometry change to the ν_1 symmetric stretch normal coordinate, shown in Fig. 8(a), suggests that excitation of this mode will occur upon photodetachment, in agreement with the present results.

Peaks B and D in the C_4^- spectrum, are located at 0.736 and 0.487 eV eKE, respectively. On the basis of *ab initio* frequency calculations alone,[58,62] peak B, located 339 ± 55 cm^{-1} from the origin, could be assigned to either the 5_0^2 or the 4_0^1 transition. The recent measurement[21(b)] of the ν_5 vibrational frequency ($\nu_5 = 172.4\ cm^{-1}$) agrees well with the A–B peak spacing. The 4_0^1 transition is symmetry forbidden within the Franck–Condon approximation, but can occur in the presence of vibronic coupling to a nearby electronic state. While this transition might normally be excluded from consideration, the strong polarization dependence of peaks B and D relative to the other peaks suggests that vibronic coupling may indeed be occurring. As observed by Ervin and Lineberger[35] in their C_2H^- photoelectron spectrum, a signature of non-Franck–Condon allowed transitions which occur only through vibronic coupling is that the polarization dependence of these peaks differs from that of the Franck–Condon allowed transitions. The 4_0^1 transition can occur if the $v_4 = 1$ level is coupled to the $v_4 = 0$ or 2 levels of a nearby Π electronic state. *Ab initio* calculations predict that a C_4

excited state of the appropriate symmetry ($^3\Pi_g$) lies just 1.00 eV above the $^3\Sigma_g^-$ ground state.[65] While the assignment of peak B to the 5_0^2 transition is certainly possible, the polarization dependence of the intensity of such a transition is difficult to explain. The assignment of peak B to the 4_0^1 transition provides a bending vibrational frequency of $\nu_4 = 339 \pm 55$ cm^{-1}. Due to its similar polarization dependence and appropriate spacing, peak D can be assigned as the $1_0^1 4_0^1$ combination band.

Although the relative intensity of peak E does not vary significantly as a function of laser polarization, it is assigned as a transition to an excited state of linear C_4 ($T_0 = 0.327 \pm 0.006$ eV). This assignment is based upon two major factors: (1) no reasonable vibrational state assignment can be made which agrees with the frequencies available from theoretical and experimental results and (2) two excited electronic states are predicted to lie in the vicinity of peak E. From the electronic configuration of linear C_4, $\ldots 1\pi_u^4 4\sigma_u^2 5\sigma_g^2 1\pi_g^2$, three electronic states can be formed: $^3\Sigma_g^-$, $^1\Sigma_g^+$, and $^1\Delta_g$. *Ab initio* calculations and high resolution gas phase absorption experiments agree that the ground state of linear C_4 is $^3\Sigma_g^-$.[24,62] Therefore, peak E can be assigned to either the $^1\Delta_g$ or the $^1\Sigma_g^+$ electronic states which have been calculated as nearly isoenergetic states lying between 0.25 and 0.75 eV.[65,66] Based upon Hund's rules and Liang *et al.*'s *ab initio* results,[67] peak E is assigned to the $^1\Delta_g$ excited state.

The 4.66 eV C_6^- photoelectron spectrum (Fig. 4), contains several partially resolved peaks to the low eKE side of the origin, peak A. A higher resolution (10 cm^{-1}) threshold photodetachment spectrum, recently obtained in our laboratory,[68] better resolves peak C, which lies 480 cm^{-1} from the origin. Based on the photoelectron spectra of the odd carbon cluster anions, it is tempting to assign peak C to excitation of the lowest frequency symmetric stretch in C_6 (the 3_0^1 transition). *Ab initio* calculations,[13,58] however, predict that the frequency of this mode is ~150–200 cm^{-1} larger than the A–C peak spacing. Alternatively, agreement is found between the A–C spacing and twice the predicted ν_7 frequency, indicating the possible assignment of peak C to the 7_0^2 transition (a π_g bending mode). While peak B, which lies 194 cm^{-1} from the origin, could be assigned to the 9_0^2 transition (a π_u bending mode) on the basis of comparison with *ab initio* values,[13,58] this peak does not appear in the threshold photodetachment spectrum. It may instead be a sequence band transition from vibrationally excited C_6^- which does not appear in the threshold spectrum because of differing ion source conditions in the two experiments; our experience with Si_2^- (Ref. 69) indicates that the source configuration in the threshold instrument produces somewhat colder ions.

Peak D, located at 0.312 eV, is 1315 cm^{-1} above the origin. This peak spacing does not agree well with calculated vibrational frequencies for linear C_6. The nearest agreement is with the ν_2 symmetric stretch (*ab initio* value[58(c)] for $\nu_2 = 1759$ cm^{-1}). In accord with this assignment, peak E is most likely a sequence band in combination with the 2_0^1 transition. It is also possible that peak D represents the transition to the $^1\Delta_g$ excited electronic state of linear C_6, predicted to lie ~1200 cm^{-1} above the ground state.[67,70]

Due to the high electron affinity of C_8 relative to C_4 and C_6, the amount of information obtained from the C_8^- spectrum is not as abundant. The spectrum (Fig. 4), contains two peaks (A and B) at very low eKE separated by ≈565 cm^{-1}. This lies close to the predicted value of the ν_4 symmetric stretch vibration in C_8,[58] so peak B is tentatively assigned to the 4_0^1 transition. It is also possible that peak B represents the $^1\Delta_g$ electronic state of C_8 (predicted[67] $T_e = 1130$ cm^{-1}) based upon the calculations by Liang *et al.*[67] which predict a decreasing $^3\Sigma_g^- - {}^1\Delta_g$ splitting as a function of increasing chain length in the linear even-numbered carbon molecules.

D. C_{10}, C_{11}, and nonlinear anion photodetachment

The photoelectron spectra of C_{10}^- and C_{11}^- (Fig. 5) have a different appearance than the other spectra presented. The C_{10}^- spectrum consists of several broad unresolved features. The C_{11}^- spectrum has similar broad features, but also exhibits three sharp peaks (labeled as A, B, and C). These three peaks taken alone strongly resemble the linear anion→linear neutral transitions seen in the C_{2n+1}^- spectra. We therefore assign peak A to the linear→linear origin and peaks B and C, spaced 440 and 830 cm^{-1}, respectively, from peak A to transitions to vibrationally excited levels of linear C_{11}. The approximately equal spacing of the three peaks suggests that they may belong to a single vibrational progression, most likely in the breathing mode analogous to the ν_4 symmetric stretch in C_9. The electron affinity determined for the linear C_{11} molecule, 3.913 ± 0.010 eV, compares well with Yang *et al.*'s[18] assignment of the linear C_{11} electron affinity as 4.00 ± 0.1 eV. The C_{10}^- spectrum, in contrast, shows no evidence for linear→linear transitions.

We next consider the broad structure in the C_{10}^- and C_{11}^- spectra. Every *ab initio* calculation for C_{10} has predicted a monocyclic ground state with the lowest linear isomer considerably higher in energy; Schaefer predicts an energy difference of 2.9 eV, for example.[71] It is therefore reasonable to assign the C_{10}^- spectrum to transitions to one or more electronic states of the cyclic C_{10} isomer. Based upon its similarity to the C_{10}^- spectrum, the broad structure in the C_{11}^- spectrum is also assigned to a transition to cyclic C_{11}. Thus, the C_{11}^- spectrum exhibits transitions to both the linear and cyclic forms of C_{11}.

A more difficult question pertains to the structures of the C_{10}^- and C_{11}^- anions which yield the broad features in the two spectra. Specifically, are these features due to linear anion→cyclic neutral transitions or cyclic anion→cyclic neutral transitions? The C_{11}^- spectrum suggests the latter to be the case. If only the linear C_{11}^- anions were responsible, then it is difficult to understand why the integrated intensity of the three sharp peaks assigned to the linear→linear transition is so much smaller than that of the broad features. A more reasonable explanation is that both the cyclic and linear isomers of C_{11}^- are present in the ion beam, and that these are responsible for the broad features and the narrow peaks, respectively, in the spectrum. Yang *et al.*[18] used similar rea-

soning to explain how their C_{11}^- photoelectron spectrum changed as a function of ion source conditions.

For C_{10} and C_{11}, the assignment of the long tails in the spectra to the cyclic anion→cyclic neutral transitions allows us to estimate the electron affinities of the cyclic molecules. Based upon the eKE at which these long tails approach base line, we can approximate the EAs of cyclic C_{10} and C_{11} to be 2.2 ± 0.1 and 1.5 ± 0.1 eV, respectively. These values are indicated by arrows in the C_{10}^- and C_{11}^- photoelectron spectra (Fig. 5).

One problem with the assignment of the broad features to the cyclic→cyclic transitions is that these features extend over at least 2 eV of electron kinetic energy, implying a substantial difference in geometry between the anion and the neutral and/or the presence of overlapping electronic transitions. Both of these possibilities appear reasonable in light of the *ab initio* study by Liang and Schaeffer,[71] which predicts three close-lying cyclic isomers of C_{10}: two cumulenic forms (one with D_{5h} symmetry and one with D_{10h} symmetry) and one acetylenic form (D_{5h}). The bond lengths and angles are quite different among these three isomers. One can therefore envision transitions between cyclic forms of the anion and neutral involving a considerable change in geometry. Whether such a change is sufficient to explain the broad features in the C_{10}^- and C_{11}^- spectra will require calculations of the anion geometries and a multidimensional Franck–Condon simulation of the spectrum.

As noted previously, the C_6^-, C_8^-, and C_5^- photoelectron spectra show low-intensity "tails" on the high eKE side of the sharp structure of the spectra (for C_5^-, the tail is only visible in the 3.49 eV spectrum). These tails extend for nearly 1 eV, suggesting that they are not simply "hot bands." Based on our interpretation of the C_{10}^- and C_{11}^- spectra, we believe that the tails are due to transitions involving cyclic forms of the anion and/or neutral molecules. *Ab initio* calculations indicate that while the cyclic and linear forms of neutral C_6 are nearly degenerate, the cyclic form of the anion lies 1.4 eV above the linear ground state.[55] This suggests that the tail in the C_6^- spectrum results from the presence of cyclic C_6^- in the ion beam, and that either cyclic→cyclic or cyclic→linear transitions are occurring. Similar explanations account for the tails in the C_5^- and C_8^- spectra.

Note that Feldman *et al.*[26] claim to observe the cyclic forms of C_5^- and C_6^- with relatively low electron binding energies in their CEI experiments. Their Cs^+ bombardment ion source lacked the cooling provided by a supersonic jet, so one might expect more higher energy cyclic anions in their experiment as compared to ours. In any case, our explanation of the tails in our photoelectron spectra is consistent with their earlier work.

The most controversial "cyclic vs linear" debate concerns the structure of C_4, as evidenced by the number of recent theoretical results cited in the discussion of the C_4^- photoelectron spectrum. Unlike the spectra of the other even-numbered carbon molecules, there is no evidence in the C_4^- spectra that a detectable number of cyclic anions are produced in our experiment. Thus, because we see no evidence for transitions to cyclic C_4, we cannot say anything about its stability relative to linear C_4.

V. CONCLUSIONS

Vibrationally resolved spectra of the carbon molecules C_2–C_{11} have been obtained using anion photoelectron spectroscopy. The spectra of C_2^-–C_9^- are dominated by transitions between the linear forms of the anions and neutrals. Electron affinities are determined for the linear isomers of C_2–C_9 and C_{11} with a typical uncertainty of ~0.010 eV. The spectra confirm the even–odd alternation of electronic structure seen by Yang *et al.*[18] In addition, several vibrational frequencies (including symmetric stretch, antisymmetric stretch, and bending modes) are determined for these linear species. The spectra of all the odd clusters show excitation of the breathing mode symmetric stretch upon photodetachment and there is a decrease in the frequency of this mode as the carbon chain length increases. The 3.49 eV photoelectron spectrum of C_5^- shows evidence for a low-lying excited electronic state. A possible transition to an excited state of C_4 is observed as well.

Several of the spectra show evidence for photodetachment transitions involving nonlinear isomers of the anion and/or neutral. The spectra of C_{10}^- and C_{11}^- show broad features which appear to result from transitions between cyclic anions and cyclic neutral clusters. For C_5^-, C_6^-, and C_8^-, the spectra suggest that a small number of cyclic anions in our ion beam are detached to form either cyclic or linear neutrals.

It is clear from these results that anion photoelectron spectroscopy can provide a wealth of information about carbon clusters. Planned experiments at higher photodetachment energy will yield a more complete picture of the low-lying excited electronic states of these species. In addition, higher resolution (6–10 cm^{-1}) investigations of carbon clusters using threshold photodetachment spectroscopy[59,69,72] are currently in progress.

ACKNOWLEDGMENTS

Support from the Office of Naval Research under Contract No. N0014-87-0495 is gratefully acknowledged. We would like to thank Dr. J. M. L. Martin and Dr. K. Raghavachari for communication of unpublished results.

[1] P. Gerhardt, S. Loffler, and K. H. Homann, Chem. Phys. Lett. **137**, 306 (1987).
[2] R. E. Honig, J. Chem. Phys. **22**, 126 (1954).
[3] P. F. Bernath, K. H. Hinkle, and J. J. Keady, Science **244**, 562 (1989).
[4] W. Krätschmer, K. Fostiropoulos, and D. R. Huffman, Chem. Phys. Lett. **170**, 167 (1990).
[5] J. M. Hawkins, A. Meyer, T. A. Lewis, S. Loren, and F. J. Hollander, Science **252**, 312 (1991).
[6] W. Weltner, Jr., and R. J. van Zee, Chem. Rev. **89**, 1713 (1989).
[7] K. S. Pitzer and E. Clementi, J. Am. Chem. Soc. **81**, 4477 (1959).
[8] R. Hoffman, Tetrahedron **22**, 521 (1966).
[9] (a) C. A. Schmuttenmaer, R. C. Cohen, N. Pugliano, J. R. Heath, A. L. Cooksy, K. L. Busarow, and R. J. Saykally, Science **249**, 897 (1990); (b) H. Sasada, T. Amano, C. Jarman, and P. F. Bernath, J. Chem. Phys. **94**, 2401 (1991).
[10] (a) J. R. Heath, A. L. Cooksy, M. H. W. Gruebele, C. A. Schmuttenmaer, and R. J. Saykally, Science **244**, 564 (1989); (b) N. Moazzen-Ahmadi, A. R. W. McKellar, and T. Amano, J. Chem. Phys. **91**, 2140 (1989); (c) Chem. Phys. Lett. **157**, 1 (1989).
[11] (a) J. R. Heath, R. A. Sheeks, A. L. Cooksy, and R. J. Saykally, Science **249**, 895 (1990); (b) J. R. Heath and R. J. Saykally, J. Chem. Phys. **94**, 1724 (1991).

[12] R. A. Whiteside, R. Krishnan, D. J. Defrees, J. A. Pople, and P. von R. Schleyer, Chem. Phys. Lett. **78**, 538 (1981).
[13] K. Raghavachari and J. S. Binkley, J. Chem. Phys. **87**, 2191 (1987).
[14] J. R. Heath and R. J. Saykally, J. Chem. Phys. **93**, 8392 (1990).
[15] K. Raghavachari, R. A. Whiteside, and J. A. Pople, J. Chem. Phys. **85**, 6623 (1986).
[16] (a) Z. Slanina, Chem. Phys. Lett. **142**, 512 (1987); (b) **173**, 164 (1990).
[17] (a) R. J. van Zee, R. F. Ferrante, K. J. Zeringue, W. Weltner, Jr., and D. W. Ewing, J. Chem. Phys. **88**, 3465 (1988); (b) R. J. van Zee, R. F. Ferrante, K. J. Zeringue, and W. Weltner, Jr., *ibid.* **86**, 5212 (1987); (c) H. M. Cheung and W. R. M. Graham, *ibid.* **91**, 6664 (1989).
[18] S. Yang, K. J. Taylor, M. J. Craycraft, J. Conceicao, C. L. Pettiette, O. Cheshnovsky, and R. E. Smalley, Chem. Phys. Lett. **144**, 431 (1988).
[19] S. H. Yang, C. L. Pettiette, J. Conceicao, O. Cheshnovsky, and R. E. Smalley, Chem. Phys. Lett. **139**, 233 (1987).
[20] K. R. Thompson, R. L. DeKock, and W. Weltner, Jr., J. Am. Chem. Soc. **93**, 4688 (1971).
[21] (a) L. N. Shen and W. R. M. Graham, J. Chem. Phys. **91**, 5115 (1989); (b) P. A. Withey, L. N. Shen, and W. R. M. Graham, *ibid.* **95**, 820 (1991); (c) L. N. Shen, P. A. Withey, and W. R. M. Graham, *ibid.* **94**, 2395 (1991).
[22] M. Vala, T. M. Chandrasekhar, J. Szczepanski, R. van Zee, and W. Weltner, Jr., J. Chem. Phys. **90**, 595 (1989).
[23] M. Vala, T. M. Chandrasekhar, J. Szczepanski, and R. Pellow, High Temp. Sci. **27**, 19 (1990).
[24] J. R. Heath and R. J. Saykally, J. Chem. Phys. **94**, 3271 (1991).
[25] One vibrational frequency is obtained for C_4, C_7, and C_9, however, Moazzen-Ahmadi *et al.* (Ref. 21) determine three frequencies for C_5, by assigning hot band transitions.
[26] (a) H. Feldman, D. Kella, E. Malkin, E. Miklazky, Z. Vager, J. Zajfman, and R. Naaman, J. Chem. Soc. Faraday Trans. **86**, 2469 (1990); (b) M. Algranati, H. Feldman, D. Kella, E. Malkin, E. Miklazky, R. Naaman, Z. Vager, and J. Zajfman, Isr. J. Chem. **30**, 79 (1990); (c) J. Chem. Phys. **90**, 4617 (1989).
[27] R. B. Metz, A. Weaver, S. E. Bradforth, T. N. Kitsopoulos, and D. M. Neumark, J. Chem. Phys. **94**, 1377 (1990).
[28] O. Cheshnovsky, S. H. Yang, C. L. Pettiette, M. J. Craycraft, and R. E. Smalley, Rev. Sci. Instrum. **58**, 2131 (1987).
[29] W. C. Wiley and I. H. McLaren, Rev. Sci. Instrum. **26**, 1150 (1955).
[30] A. Weaver, D. W. Arnold, S. E. Bradforth, and D. M. Neumark, J. Chem. Phys. **94**, 1740 (1991).
[31] (a) E. A. Ballik and D. A. Ramsay, Astrophys. J. **137**, 84 (1963); (b) **137**, 61 (1963).
[32] K. P. Huber and G. Herzberg, *Molecular Spectra and Molecular Structure IV: Constants of Diatomic Molecules* (Van Nostrand–Reinhold, New York, 1977).
[33] (a) K. Kawaguchi, K. Matsumura, H. Kanamori, and E. Hirota, J. Chem. Phys. **91**, 1953 (1989); (b) G. W. Lemire, Z. Fu, Y. M. Hamrick, S. Taylor, and M. D. Morse, J. Phys. Chem. **93**, 2313 (1989); (c) L. Gausset, G. Herzberg, A. Lagerqvist, and B. Rosen, Discuss. Faraday Soc. **35**, 113 (1963).
[34] J. M. Oakes and G. B. Ellison, Tetrahedron **42**, 6263 (1986).
[35] K. M. Ervin and W. C. Lineberger, J. Phys. Chem. **95**, 1167 (1991).
[36] J. W. Rabalais, *Principles of Ultraviolet Photoelectron Spectroscopy* (Wiley, New York, 1977).
[37] For a full list of references, see Weltner and van Zee review, Ref. 6.
[38] (a) W. C. Lineberger and T. A. Patterson, Chem. Phys. Lett. **13**, 40 (1972); (b) G. Herzberg and A. Lagerqvist, Can. J. Phys. **46**, 2363 (1968).
[39] (a) R. D. Mead, U. Hefter, P. A. Schultz, and W. C. Lineberger, J. Chem. Phys. **82**, 1723 (1985); (b) B. D. Rehfuss, D. J. Liu, B. M. Dinelli, M. F. Jagod, W. C. Ho, M. W. Crofton, and T. Oka, *ibid.* **89**, 129 (1988).
[40] This corrected the previous value measured from autodetachment experiments; P. L. Jones, R. D. Mead, B. E. Kohler, S. D. Rosner, and W. C. Lineberger, J. Chem. Phys. **73**, 4419 (1980).
[41] P. Rosmus and H. Werner, J. Chem. Phys. **80**, 5085 (1984).
[42] K. Raghavachari, Chem. Phys. Lett. **171**, 249 (1990).
[43] A. J. Merer, Can. J. Phys. **45**, 4103 (1967).
[44] W. Weltner, Jr., and D. McLeod, Jr., J. Chem. Phys. **40**, 1305 (1964).
[45] E. A. Rohlfing, J. Chem. Phys. **91**, 4531 (1989).
[46] M. Polak, M. Gilles, and C. Lineberger (private communication).
[47] L. Gausset, G. Herzberg, A. Lagerqvist, and B. Rosen, Astrophys. J. **142**, 45 (1965).
[48] (a) F. J. Northrup and T. J. Sears, J. Opt. Soc. Am. B **7**, 1924 (1990); (b) E. A. Rohlfing and J. E. M. Goldsmith, *ibid.* **7**, 1915 (1990).
[49] While the bending mode of C_3^- is Renner–Teller active (as are the bending modes for all the carbon anions), no consideration is made for this effect in the simulations. Rather, the ν_2 mode is considered as a doubly degenerate harmonic oscillator with a frequency set at approximately the average of the frequencies calculated in Ref. 42.
[50] Time-dependent wave packet propagation technique is employed using the surface described. For further details, see, S. E. Bradforth, A. Weaver, D. W. Arnold, R. B. Metz, and D. M. Neumark, J. Chem. Phys. **92**, 7205 (1990).
[51] Morse Oscillator Rigid Bender Internal Dynamics.
[52] (a) P. Jensen, Collect. Czech. Chem. Commun. **54**, 1209 (1989); (b) J. Mol. Spectrosc. **128**, 478 (1988).
[53] V. E. Bondybey and J. H. English, J. Chem. Phys. **68**, 4641 (1978).
[54] J. Perić-Radić, J. Römelt, S. D. Peyerimhoff, and R. J. Buenker, Chem. Phys. Lett. **50**, 344 (1977).
[55] K. Raghavachari, Z. Phys. D **12**, 61 (1989).
[56] L. Adamowicz, J. Chem. Phys. **93**, 6685 (1990).
[57] The tail appears in the 3.49 eV spectrum as a result of better sensitivity and improved resolution at lower *eKE*.
[58] (a) J. Kurtz and L. Adamowicz, Astrophys. J. **370**, 784 (1991); (b) J. M. L. Martin, J. P. François, and R. Gijbels, J. Comp. Chem. **12**, 52 (1991); (c) J. Chem. Phys. **93**, 8850 (1990).
[59] T. N. Kitsopoulos, C. J. Chick, Y. Zhao, and D. M. Neumark, J. Chem. Phys. J. Chem. Phys. **95**, 5479 (1991).
[60] J. W. Berkowitz, *Photoabsorption, Photoionization and Photoelectron Spectroscopy* (Academic, New York, 1979), pp. 155–357.
[61] (a) J. M. L. Martin (private communication); (b) K. Raghavachari (private communication).
[62] J. M. L. Martin, J. P. François, and R. Gijbels, J. Chem. Phys. **94**, 3753 (1991).
[63] V. Parasuk and J. Almlöf, J. Chem. Phys. **94**, 8172 (1991).
[64] J. D. Watts, I. Cernusak, and R. J. Bartlett, Chem. Phys. Lett. **178**, 259 (1991).
[65] G. Pacchioni and J. Koutecký, J. Chem. Phys. **88**, 1066 (1988).
[66] (a) D. H. Magers, R. J. Harrison, and R. J. Bartlett, J. Chem. Phys. **84**, 3284 (1986); (b) A. V. Nemukhin, N. F. Stepanov, and A. A. Safonov, Teor. Eksp. Khim. **18**, 608 (1982).
[67] C. Liang and H. F. Schaefer III, Chem. Phys. Lett. **169**, 150 (1990).
[68] C. J. Chick, Y. Zhao, T. N. Kitsopoulos, and D. M. Neumark (unpublished).
[69] T. N. Kitsopoulos, C. J. Chick, Y. Zhao, and D. M. Neumark, J. Chem. Phys. **95**, 1441 (1991).
[70] V. Parasuk and J. Almlöf, J. Chem. Phys. **91**, 1137 (1989).
[71] C. Liang and H. F. Schaefer III, J. Chem. Phys. **93**, 8844 (1990).
[72] T. N. Kitsopoulos, I. M. Waller, J. G. Loeser, and D. M. Neumark, Chem. Phys. Lett. **159**, 300 (1989).